

# Thermal Stability and Crystallization Behaviour of Modified ABS/PP Nanocomposites

Marianna I. Triantou, Petroula A. Tarantili

**Abstract**—In this research work, poly (acrylonitrile-butadiene-styrene)/polypropylene (ABS/PP) blends were processed by melt compounding in a twin-screw extruder. Upgrading of the thermal characteristics of the obtained materials was attempted by the incorporation of organically modified montmorillonite (OMMT), as well as, by the addition of two types of compatibilizers; polypropylene grafted with maleic anhydride (PP-g-MAH) and ABS grafted with maleic anhydride (ABS-g-MAH). The effect of the above treatments was investigated separately and in combination. Increasing the PP content in ABS matrix seems to increase the thermal stability of their blend and the glass transition temperature ( $T_g$ ) of SAN phase of ABS. From the other part, the addition of ABS to PP promotes the formation of its  $\beta$ -phase, which is maximum at 30 wt% ABS concentration, and increases the crystallization temperature ( $T_c$ ) of PP. In addition, it increases the crystallization rate of PP. The  $\beta$ -phase of PP in ABS/PP blends is reduced by the addition of compatibilizers or/and organoclay reinforcement. The incorporation of compatibilizers increases the thermal stability of PP and reduces its melting ( $\Delta H_m$ ) and crystallization ( $\Delta H_c$ ) enthalpies. Furthermore it decreases slightly the  $T_g$ s of PP and SAN phases of ABS/PP blends. Regarding the storage modulus of the ABS/PP blends, it presents a change in their behavior at about 10°C and return to their initial behavior at 110°C. The incorporation of OMMT to no compatibilized and compatibilized ABS/PP blends enhances their storage modulus.

**Keywords**—Acrylonitrile, butadiene, styrene terpolymer, compatibilizer, organoclay, polypropylene.

## I. INTRODUCTION

POLYPROPYLENE, PP, is a semicrystalline thermoplastic and one of the most widely used commodity polymers [1], [2]. It is characterized by good elongation, high heat distortion temperature, good heat and chemical resistance, good electrical properties, good processability and economic merits [1]-[5]. Also, it is lightweight and easily fabricated [6]. However, the use of the PP is restricted by the low impact strength and high molding shrinkage [4]-[6].

On the other hand, the poly (acrylonitrile-butadiene-styrene) terpolymer, ABS, is one of the most popular, amorphous, engineering thermoplastics [6]. In all classical ABS molding compounds, the continuous phase (matrix) consists of copolymers of styrene (or alkylstyrene) and acrylonitrile, whereas butadiene forms the dispersed phase. Regarding its properties, ABS presents poor elongation, but good impact strength, chemical resistance, easy processing and fine surface appearance [2], [6], [7].

M. I. Triantou is with the National Technical University of Athens, Zographou, 15780 Greece (e-mail: mtriantou@teemail.gr).

P. A. Tarantili is with the National Technical University of Athens, Zographou, 15780 Greece (phone: +30 2107723289; fax: +30 2107723163; e-mail: taran@chemeng.ntua.gr).

Polymer blending has been considered as an effective method for the development of new polymeric materials [3]. Hence, blending of PP with ABS would be desirable to achieve higher impact strength without losing additional positive properties of each polymer and, moreover, widening its scope of applications [2].

Unfortunately, most of the polymer blends are found to be immiscible due to difference in viscoelastic properties, surface tension and intermolecular interactions [8]. Melt blends of PP with ABS are incompatible since the two polymers differ considerably in polarity, solubility parameter and interfacial tension leading to poor mechanical properties [1]. To reduce surface tension and to increase molecular interactions, a third component known as a compatibilizer is often used [8]. The prime consideration when one selects a compatibiliser is to use one whose segments are chemically identical to the homopolymer phases or at least strongly interact with those phases [1].

Furthermore, it has been reported that organoclays can contribute to compatibility of blends of immiscible polymers, acting as linkages between the two phases by embedding in both of them and, hence, improve their properties [9]-[11]. Polymer/ organic layered silicate nanoparticles have better properties compared to the traditional polymer composites, such as mechanical, thermal and optical properties as well as improved processability [6]. By the addition of the clay in the polymers, the morphology can be affected by several factors such as the composition of the dispersed phase, viscosity ratio and the elasticity of each phase [12]. The dispersion of the clay is influenced by the polarity of the polymers [12].

## II. EXPERIMENTAL

### A. Materials

The terpolymerpoly (acrylonitrile – butadiene – styrene) was supplied by BASF, under the trade name Terluran® GP-35, whereas the polypropylene (Ecolen® HZ40P) was donated by Hellenic Petroleum. In addition, two types of compatibilizers; polypropylene grafted with maleic anhydride, PP-g-MAH (Fusabond P353) supplied by DuPont™ and poly(acrylonitrile – butadiene – styrene) grafted with maleic anhydride, ABS-g-MAH (GPM400AB) supplied by Ningbo Nengzhiguang New Materials Technology Co., Ltd. were tested in ABS/PP blends at concentration of 10 wt%. Commercial montmorillonite clay with the trade name Cloisite® 30B, supplied by Rockwood Clay Additives GmbH, was also incorporated as reinforcing nanofiller in order to prepare nanocomposites at concentrations of 2 phr.

### B. Preparation of Nanocomposites

ABS/PP blends with compositions: 100/0, 70/30, 50/50, 30/70 and 0/100 (w/w) were prepared in a co-rotating twin-screw extruder, with L/D=25 and 16 mm diameter (Haake PTW 16). The rotational speed of screws was 200 rpm. The extruder was heated at five zones along the cylinder and the die. The temperature profiles of the barrel from the hopper to the die were 190-195-195-200-200-205°C for ABS blends, 180-180-185-185-190-190°C for PP blends and 190-190-195-195-200-200°C for ABS/PP blends. All materials were dried before processing, in order to avoid hydrolytical degradation. After melt mixing, the obtained material in the form of continuous strands was granulated using a Brabender knife pelletizer.

### C. Characterization

Thermogravimetric analysis (TGA) measurements were performed in a Mettler Toledo (TGA-DTA model) thermal gravimetric analyzer. The tests were taken place with samples of 8-10 mg from 25 to 600°C, at a heating rate of 10°C/min, under nitrogen.

Differential Scanning Calorimetry (DSC) measurements were run in a Mettler Toledo model DSC 1 differential scanning calorimeter. For the non-isothermal crystallization process, the samples were heated from 30 to 200°C and maintain at this temperature for little time to erase previous thermal history and then were cooled to 30°C and heated again to 200°C, at a rate of 10°C/min. For the isothermal crystallization process, the samples were heated from 30 to 200°C at a heating rate of 50°C/min and maintained at 200°C for 5 min to erase any thermal history. Then the samples were cooled toward to a predetermined temperature at cooling rate of 20°C/min and maintained at this temperature for enough time to leave the sample crystallization completely. Subsequently, the samples were heated again to 200°C at a heating rate of 10°C/min. The weight of samples was between 8-10 mg. All DSC measurements were carried out in nitrogen atmosphere.

The crystallization behavior of PP and its blends was evaluated in a Siemens 5000 apparatus X-ray diffractometer (40kV, 30mA) using CuK $\alpha$  irradiation with a wavelength of  $\lambda=0.154$  nm. The diffractograms were scanned in the  $2\theta$  range from 2-40° with rate of 0.02°/sec. Samples for X-ray analysis were obtained from compression molded plaques.

Dynamic mechanical analysis (DMA) measurements were carried out in an Anton Paar (model MCR 301) dynamic mechanical analyzer at a frequency of 1 Hz, with a heating rate of 5°C/min between -120 and 160°C. Samples prepared by injection molding were studied by this technique. Injection moulding was performed with an ARBURG 221K ALLROUNDER machine. For ABS, the temperature profile was: 260-260-260-260-265°C, with 1000 and 1150 bar injection pressures and 500 bar back pressure. For all the other ABS/PP blends, the temperature profile was: 190-190-190-195-195°C, with 1400 and 1350 bar injection pressures and 600 bar back pressure.

## III. RESULTS AND DISCUSSION

According to thermogravimetric analysis (TGA), PP exhibits higher thermal stability compared to ABS. The thermal degradation mechanism of their blends takes place in two stages with the first one corresponding to the thermal degradation of ABS phase and the second one to that of PP phase (Fig. 1).

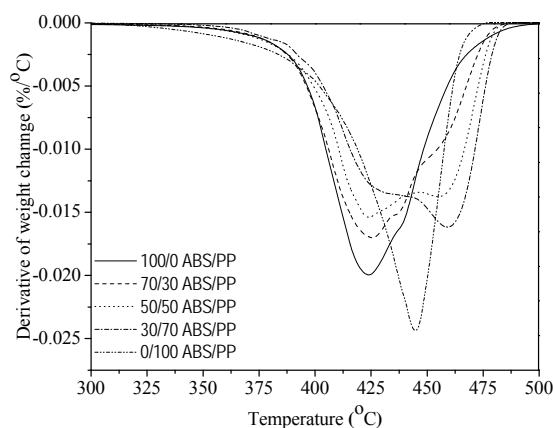


Fig. 1 Derivative of weight change versus temperature, for no compatibilized ABS/PP blends

From Table I, it is observed that the ABS/PP blends at 70/30 and 50/50 w/w present similar values of onset degradation temperature ( $T_{onset}$ ) with that of pure ABS. The addition of PP-g-MAH or ABS-g-MAH in PP causes increase of its  $T_{onset}$ , whereas does not have any significant effect in  $T_{onset}$  of ABS/PP blends. The incorporation of nanofiller in no compatibilized and compatibilized ABS/PP blends does not affect sensibly the  $T_{onset}$ .

TABLE I  
ONSET DEGRADATION TEMPERATURE OF ABS/PP BLENDS

Comp. (10%)	clay (phr)	$T_{onset}$ (°C)				
		ABS/PP (w/w)				
		100/0	70/30	50/50	30/70	0/100
-	0	401.6 $\pm 1.14$	399.8 $\pm 1.54$	402.9 $\pm 1.02$	412.9 $\pm 0.05$	422.4 $\pm 3.39$
	2	402.2 $\pm 0.84$	401.5 $\pm 0.18$	403.5 $\pm 0.56$	411.9 $\pm 1.22$	425.2 $\pm 0.66$
	0	-	400.1 $\pm 0.39$	405.3 $\pm 2.46$	412.7 $\pm 0.44$	429.7 $\pm 1.81$
	2	-	402.5 $\pm 0.42$	404.5 $\pm 0.08$	409.2 $\pm 0.68$	428.1 $\pm 0.47$
PP-g-MAH	0	398.6 $\pm 0.51$	400.0 $\pm 0.46$	403.1 $\pm 0.57$	413.1 $\pm 0.73$	427.8 $\pm 2.28$
	2	399.7 $\pm 0.05$	400.8 $\pm 0.09$	404.0 $\pm 1.48$	413.3 $\pm 0.93$	427.7 $\pm 2.56$
	0	398.6 $\pm 0.51$	400.0 $\pm 0.46$	403.1 $\pm 0.57$	413.1 $\pm 0.73$	427.8 $\pm 2.28$
	2	399.7 $\pm 0.05$	400.8 $\pm 0.09$	404.0 $\pm 1.48$	413.3 $\pm 0.93$	427.7 $\pm 2.56$
vPP-g-MAH		425.5 $\pm 0.01$		vABS-g-MAH		404.7 $\pm 1.60$

From Table II, it is concluded that the 30/70 w/w ABS/PP blends present the higher temperature of maximum degradation rate,  $T_{peak}$  even than that of pure PP. The addition of PP-g-MAH in ABS/PP blends does not affect significantly the measured  $T_{peak}$  values. The incorporation of ABS-g-MAH increases significantly the  $T_{peak}$  of pure PP. The incorporation of Cloisite 30B tends to increase the  $T_{peak}$  corresponded to

ABS phase in ABS-rich ABS/PP blends, whereas decreases slightly the  $T_{\text{peak}}$  corresponded to PP phase in PP-rich ABS/PP blends.

TABLE II  
MAXIMUM DEGRADATION RATE TEMPERATURE OF ABS/PP BLENDS

Comp. (10%)	clay (phr)	$T_{\text{peak}}$ (°C)				
		ABS/PP (w/w)				
		100/0	70/30	50/50	30/70	0/100
-	0	423.6 ±0.23	424.1 ±1.27	424.2/456.5 ±0.29/2.10	458.0 ±1.64	445.1 ±3.41
	2	425.3 ±0.23	425.1 ±0.23	427.2/453.6 ±0.86/0.54	454.7 ±1.66	435.5 ±1.65
PP-g- MAH	0	-	423.4 ±1.81	424.0/458.2 ±0.86/0.08	457.4 ±1.60	439.7 ±3.75
	2	-	427.1 ±0.23	430.6 ±0.78	451.5 ±0.11	438.0 ±0.86
ABS- g- MAH	0	422.2 ±1.17	425.1 ±1.02	429.6/458.0 ±0.85/0.36	460.1 ±0.32	460.5 ±1.07
	2	423.1 ±0.30	425.8 ±0.30	428.7/454.7 ±1.29/2.08	459.1 ±0.52	463.8 ±3.39
vPP-g-MAH		450.9±0.09		vABS-g-MAH		441.4±0.81

Isotactic polypropylene (iPP) has several crystalline forms: monoclinic  $\alpha$ -form ( $\alpha$ -iPP), trigonal  $\beta$ -form ( $\beta$ -iPP), orthorhombic  $\gamma$ -form ( $\gamma$ -iPP) and smectic form. Among them, the most widely occurring is the  $\alpha$ -form, which occurs under common processing conditions and is more stable than the  $\beta$ -form thermodynamically [13]. The  $\beta$ -form exhibits unique characteristics, including improved toughness, elongation at break, impact strength and higher heat distortion temperature but the yield strength and elastic modulus of  $\beta$ -PP are lower than those of  $\alpha$ -PP [13], [14]. It is obtained under some special conditions, such as quenching the melt to a certain temperature, directional crystallization in a temperature gradient field, shearing or elongation of melt during crystallization, vibration-induced crystallization or using a  $\beta$ -nucleating agent [13].

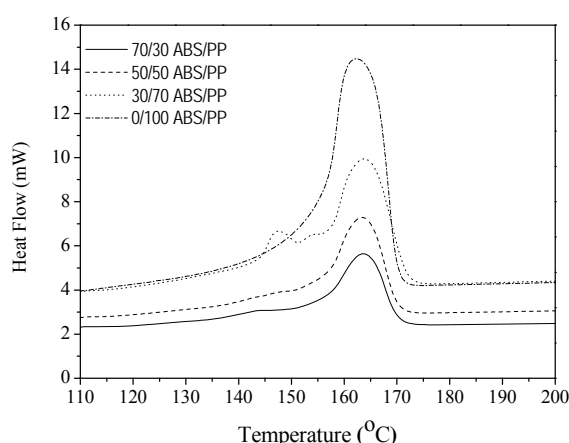


Fig. 2 DSC heating thermograms of no-compatible ABS/PP blends

Fig. 2 reveals the existence of a double melting peak for 30/70 ABS/PP blends. The melting peak at 163°C is due to  $\alpha$ -iPP and at 147°C to  $\beta$ -iPP. Therefore, it seems that ABS induces  $\beta$ -iPP crystallization ability. Wang et al. [14] observed

three melting peaks in  $\beta$ -nucleated PP/ABS blends; one strong at 150°C due to the fusion of  $\beta$ -crystal and the others at 162 and 168°C corresponded to the fusion of  $\alpha_1$  and  $\alpha_2$  crystal respectively.

The existence of  $\beta$ -iPP in ABS/PP blends was confirmed by XRD analysis (Fig. 3). It is well known that the  $\alpha$ -phase has peaks that appear at diffraction angles  $2\theta$  of 14°, 16.8°, 18.6°, 21.2° and 21.9° corresponding to the 110, 040, 130, 111 and the 131 and 040 lattice planes respectively [13]. All the patterns of pure PP and ABS/PP blends present the above diffraction peaks. However, the pure PP and PP-rich blends with ABS present a peak appeared at  $2\theta=16.2^\circ$ , which corresponds to the 300 lattice plane of  $\beta$ -crystals. Similar observations are reported by Shu et al. [13] who attributed the  $\beta$ -iPP crystallization ability of ABS to its special molecular structure containing polybutadiene blocks and SAN.

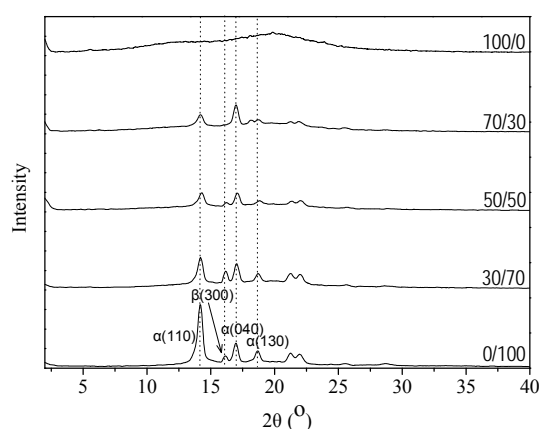


Fig. 3 XRD patterns of ABS/PP blends

Also, it is seen that as the ABS content in the ABS/PP blends increases, the amount of  $\beta$ -iPP is reduced. The intensity of peak corresponding to  $\beta$ -iPP of 30/70 ABS/PP blends is higher than that of neat PP and 50/50 w/w ABS/PP blend. This is obvious from Table III, where the content of  $\beta$ -PP in ABS/PP blends ( $k_\beta$ ) value is calculated from X-ray diffractograms according to the equation proposed by Turner-Jones et al. [14]:

$$k_\beta = \frac{H_{\beta(300)}}{H_{\alpha(110)} + H_{\alpha(040)} + H_{\alpha(130)} + H_{\beta(300)}} \quad (1)$$

where  $H_{\alpha(110)}$ ,  $H_{\alpha(040)}$  and  $H_{\alpha(130)}$  are the intensities of  $\alpha$ -diffraction peaks corresponding to angles  $2\theta$  equals to 14°, 16.8°, 18.6° respectively and  $H_{\beta(300)}$  is the intensity of  $\beta$ -diffraction peak at  $2\theta$  equal to 16.2°. From Table III, it is observed that the  $k_\beta$  value increases when 30 wt% ABS is added to the PP matrix, whereas the further addition of ABS at 50 wt% concentration decreases the investigated value which remains higher than the corresponding in pure PP. In 70/30 w/w ABS/PP blend, the  $\beta$ -diffraction peak was not detected.

Shu et al. [13] found out that the  $\beta$ -iPP amount in the blends increases with the addition of ABS and reaches its maximum

when the ABS content is 20%. They suggested that when ABS is the poor phase, the  $\beta$ -iPP can be induced in and grown from the two-phase interface. With the increase of ABS, although the  $\beta$ -iPP can be induced, the growth of crystal may be hampered by the large ABS phase domain, which causes the decrease of  $\beta$ -iPP amount. Also, they discovered that the formation of  $\beta$ -iPP in the PP/ABS blends depends not only on the induction by ABS, but also on their thermomechanical history. The degradation favors the formation of  $\alpha$ -iPP and is against the  $\beta$ -iPP in the blend.

TABLE III  
 $K_\beta$  VALUES OF ABS/PP BLENDS

Comp. (10%)	clay (phr)	$k_\beta$			
		ABS/PP (w/w)			
		70/30	50/50	30/70	0/100
-	0	-	0.16	0.22	0.11
	2	-	0.14	0.13	0.14
PP-g-MAH	0	-	0.13	0.12	0.06
	2	-	0	0	0.10
ABS-g-MAH	0	-	0.16	0.21	0.10
	2	-	0	0.15	0.10

The addition of PP-g-MAH reduces the  $k_\beta$  value at all examined proportions, mainly at 30/70 w/w ABS/PP, whereas no effect was observed by the addition of ABS-g-MAH (Fig. 4, Table III). The incorporation of organoplatelets to 50/50 and 30/70 w/w ABS/PP blends decreases the  $\beta$ -phase of PP or eliminates totally its formation. An opposite effect is observed in case of PP, where the addition of nanoclay increases the  $\beta$ -phase content.

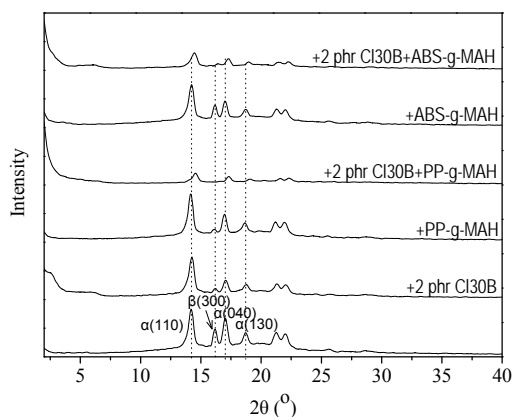


Fig. 4 XRD patterns of 30/70 ABS/PP blends

As it can be seen from Table IV, the ABS/PP blends present higher crystallization temperature,  $T_c$ , than that of pure PP. The addition of PP-g-MAH in ABS/PP blends tends to increase the  $T_c$ , whereas the incorporation of nanoparticles tends to decrease it. Shu et al. [13] observed that the total crystallinity of the blends increases as the ABS content increases up to 15 wt%. Further addition of ABS reduces the iPP crystallinity which becomes lower than that of pure PP when ABS is added at concentration higher than 30 wt% due

to the increased domain size of ABS. Xiang-Fang et al. [6] found out that the incorporation of organoclay reduces the velocity of crystallization, but increases the crystallinity.

TABLE IV  
CRYSTALLIZATION TEMPERATURE OF ABS/PP BLENDS

Comp. (10%)	clay (phr)	$T_c$ (°C)			
		ABS/PP (w/w)			
		70/30	50/50	30/70	0/100
-	0	116.5 ±0.20	117.1 ±0.24	116.5 ±0.70	113.8 ±1.34
	2	115.7 ±0.01	116.5 ±0.30	115.3 ±0.74	113.9 ±0.82
PP-g-MAH	0	118.8 ±0.37	118.3 ±0.13	117.6 ±0.14	111.5 ±0.21
	2	116.7 ±0.01	117.6 ±0.57	119.5 ±0.98	111.9 ±1.53
ABS-g-MAH	0	117.3 ±0.75	117.3 ±0.42	116.8 ±0.18	115.0 ±0.28
	2	115.7 ±0.24	116.3 ±0.75	115.5 ±0.10	115.1 ±0.35
vPP-g-MAH		92.1±0.14			

The melt temperature,  $T_m$ , does not seem to depend on the proportion of the two polymers and changes negligibly by the addition of compatibilizers or organoclay. The melting enthalpy,  $\Delta H_m$ , increases as the PP content in the investigated blend increases. The addition of PP-g-MAH to ABS/PP blends does not affect their melting enthalpy, except that of pure PP which is decreased (Table V). Furthermore, the incorporation of ABS-g-MAH or organoclay reduces the melting enthalpy. The maximum reduction occurred when ABS-g-MAH and organoclay reinforcement are combined together in the ABS/PP blends. Similar behavior presents and the crystallization enthalpy,  $\Delta H_c$ .

TABLE V  
MELTING ENTHALPY OF ABS/PP BLENDS

Comp. (10%)	clay (phr)	$\Delta H_m$ (°C)			
		ABS/PP (w/w)			
		70/30	50/50	30/70	0/100
-	0	32.14 ±1.44	45.95 ±0.65	64.03 ±0.70	93.48 ±1.02
	2	27.79 ±1.51	44.32 ±0.58	61.19 ±0.70	92.41 ±1.26
PP-g-MAH	0	31.50 ±0.71	46.08 ±0.52	64.03 ±0.33	88.46 ±0.64
	2	23.41 ±2.21	45.79 ±0.57	61.67 ±1.50	80.40 ±1.67
ABS-g-MAH	0	24.93 ±1.01	40.52 ±0.37	58.73 ±0.72	79.81 ±1.75
	2	22.13 ±0.33	39.61 ±0.17	56.44 ±0.65	76.91 ±0.37
vPP-g-MAH		52.79±0.31			

Fig. 5 shows the DSC heat flow curves of PP isothermally crystallized at 125 and 130°C. It can be seen that at higher crystallization temperature ( $T_c$ ), the peak is broader, indicating a lower crystallization rate. The maximum crystallization rate, corresponding to the peak of heat flow curve, shifts to greater crystallization time. The addition of ABS in PP matrix causes the completion of crystallization process of PP in shorter time.

An ABS/PP blend can be considered as a triple phase

mixture of styrene-acrylonitrile copolymer (SAN), butadiene rubber (PB) and polypropylene (PP). The glass transition temperature ( $T_g$ ) of each phase was detected using the dynamic mechanical analysis (DMA) and more specially by the plot of  $G''$  versus temperature. The different  $T_g$ s for each phase indicate lack of miscibility between the components of ABS/PP blend.

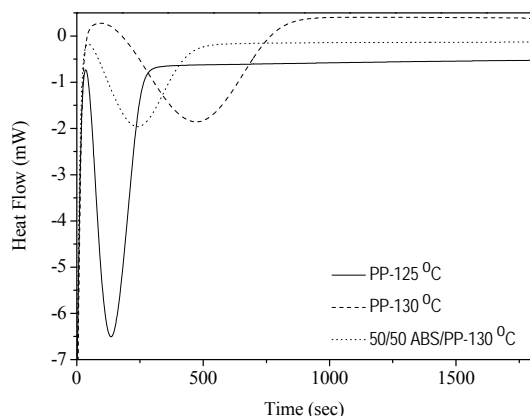


Fig. 5 DSC curves of isothermally crystallized samples

The  $T_g$  of polybutadiene phase in ABS/PP blends decreases slightly in comparison to pure ABS (Table VI). The addition of compatibilizers or/and nanoparticles in ABS/PP blends does not cause any significant change to the  $T_g$  of this phase.

TABLE VI  
GLASS TRANSITION TEMPERATURE OF ABS/PP BLENDS

Comp. (10%)	clay (phr)	T <sub>g</sub> (°C)				
		ABS/PP (w/w)				
		100/0	70/30	50/50	30/70	0/100
PB phase						
-	0	-83.0	-86.8	-84.7	-86.6	-
	2	-84.0	-87.8	-86.9	-87.5	-
PP-g-MAH	0	-	-86.4	-86.4	-86.7	-
	2	-	-86.7	-86.7	-86.7	-
ABS-g-MAH	0	-83.4	-87.2	-86.0	-85.5	-77.3
	2	-85.6	-87.0	-86.9	-86.0	-76.3
PP phase						
-	0	-	0.5	1.3	1.3	1.7
	2	-	0.3	-0.1	1.4	1.7
PP-g-MAH	0	-	-4.2	-2.3	-0.6	0.5
	2	-	-2.8	-2.6	-2.2	-0.4
ABS-g-MAH	0	-	0.0	0.0	0.6	1.4
	2	-	0.2	0.4	0.0	1.4
SAN phase						
-	0	98.5	103.7	103.9	105.2	-
	2	98.8	103.5	103.7	106.2	-
PP-g-MAH	0	-	100.1	101.8	105.6	-
	2	-	103.1	103.7	104.6	-
ABS-g-MAH	0	99.9	101.9	102.4	104.7	107.2
	2	99.3	102.4	103.7	104.7	106.8

Furthermore, the  $T_g$  of PP is found at  $\sim 2^\circ\text{C}$ , whereas that of pure SAN emerges at  $99^\circ\text{C}$ . A shift of a few degrees can be

observed for both  $T_g$ s and, more specifically, the first transition takes place at a temperature slightly lower than that of pure PP and further shifts to lower temperatures as the PP content in the blend decreases. The second transition of the blend appears at a temperature slightly higher than that of SAN phase of ABS and further increases, as the PP content increases. It also should be noted that the shift of  $T_g$  is much more enhanced for ABS, where an increase from  $98.5$  to  $105.2^\circ\text{C}$  is recorded.

The addition of compatibilizers in ABS/PP blends reduces slightly the  $T_g$  of SAN phase of ABS. Moreover, the PP-g-MAH decreases the  $T_g$  of PP phase in ABS/PP blends and more intensively when ABS content is increased. However, the incorporation of organoclay to ABS/PP blends does not have any obvious effect on the  $T_g$ s of SAN and PP phase. The combined incorporation of PP-g-MAH and nanoparticles to ABS/PP blends decreases slightly the  $T_g$  value of the PP phase.

The storage modulus,  $G'$ , is one of the most important parameters determined by DMA, relevant to the elastic response during the sample's deformation. From Fig. 6 it is observed that the  $G'$  of ABS drops sharply with increasing temperature, starting from the temperature range of  $\sim 70^\circ\text{C}$  and approaches zero at  $110^\circ\text{C}$ , while  $G'$  of PP starts to drop at  $\sim (-20)^\circ\text{C}$  and then sharply decreases approaching zero at  $150^\circ\text{C}$ . A change in the behavior of storage modulus of ABS/PP blends is recorded at about  $10^\circ\text{C}$ . In particular, below  $10^\circ\text{C}$ , the ABS/PP blends present higher storage modulus than that of neat ABS and lower than or equal to that of neat PP. On the contrary, over  $10^\circ\text{C}$ , the  $G'$  of ABS/PP blend is higher than that of neat PP and lower than that of neat ABS. Reversion to the initial behavior is noted at  $110^\circ\text{C}$ .

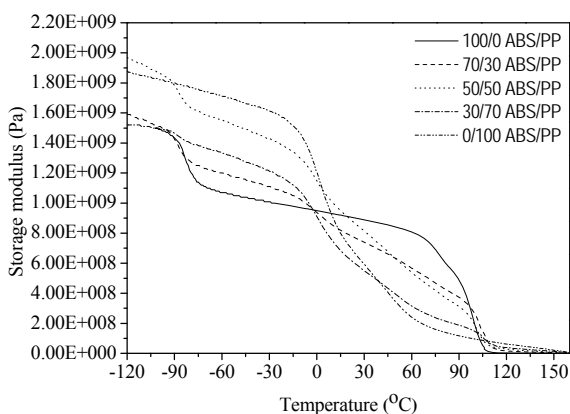


Fig. 6 Storage modulus ( $G'$ ) versus temperature of ABS/PP blends

The addition of ABS-g-MAH in ABS/PP blends increases slightly their  $G'$ , mainly at low temperatures (Fig. 7), whereas that of PP-g-MAH does not cause any positive effect in this value, except in 30/70 ABS/PP blend and pure PP. From Fig. 7, it can be seen that the incorporation of nanoparticles leads to an impressive increase of storage modulus, in comparison with this corresponding to unreinforced blends. Cai et al. [15]

found that incorporation and efficient dispersion of silicate clays increase remarkably the storage modulus of ABS nanocomposites. Ma et al. [16] observed that for nanocomposites of ABS and ABS-g-MAH, there is a significant enhancement of the storage modulus, because of the reinforcing effect of organoclay with particles of large aspect ratio. The simultaneous incorporation of reinforcing filler and compatibilizer in the examined blends leads to improvement of storage modulus. The highest value is recorded for Cloisite 30B/ABS/PP and Cloisite 30B/ABS/PP/ABS-g-MAH nanocomposites.

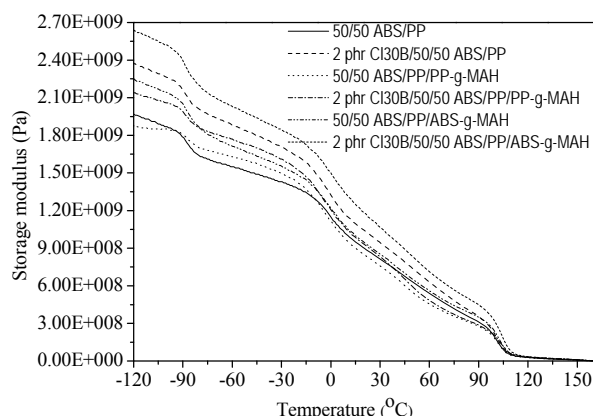


Fig. 7 Storage modulus ( $G'$ ) versus temperature of 50/50 w/w ABS/PP blends

#### IV. CONCLUSION

ABS/PP blends are usually used in electrical and electronic equipment. The addition of PP improves the thermal stability of ABS and a two-stage thermal degradation mechanism is recorded for their blends. The 30/70 w/w ABS/PP blend present higher temperature of maximum degradation rate, even than that of pure PP, maybe due to the higher amount of  $\beta$ -PP in this proportion of blend. The ABS/PP blends present higher crystallization temperature than that of pure PP and their crystallization enthalpy and melting enthalpy increase as the PP content in the investigated blends increases. The incorporation of nanoparticles to no compatibilized and compatibilized ABS/PP blends leads to an impressive increase of their storage modulus.

The slight increase of  $T_g$  of SAN phase of ABS in ABS/PP blend with increasing PP content is more intense than the decrease of the  $T_g$  of PP phase with increasing the ABS concentration. Regarding the storage modulus, the ABS/PP blends present a change in their behavior at about 10°C. The incorporation of nanoparticles to no compatibilized and compatibilized ABS/PP blends leads to an impressive increase of their storage modulus.

#### ACKNOWLEDGMENT

We would like to acknowledge the Bodossaki Foundation for its financial support.

#### REFERENCES

- [1] M. Frounchi, R. P. Burford, "State of compatibility in crystalline polypropylene/ABS amorphous terpolymer thermoplastic blends. Effect of styrenic copolymers as compatibilizers", *Iran. J. Polym. Sci. Technol.*, vol. 2, no. 2, pp. 59-68, 1993.
- [2] Y. K. Lee, J. B. Lee, D. H. Park, W. N. Kim, "Effects of accelerated aging and compatibilizers on the mechanical and morphological properties of polypropylene and poly(acrylonitrile-butadiene-styrene) blends", *J. Appl. Polym. Sci.*, vol. 127, issue 2, pp. 1032-1037, 2013.
- [3] H. G. Lee, Y.-T. Sung, Y. K. Lee, W. N. Kim, H. G. Yoon, H. S. Lee, "Effects of PP-g-MAH on the mechanical, morphological and rheological properties of polypropylene and poly(acrylonitrile-butadiene-styrene) blends", *Macromol. Res.*, vol. 17, no. 6, pp. 417-423, 2009.
- [4] A. C. Patel, R. B. Brahmabhatt, B. D. Sarawade, S. Devi, "Morphological and mechanical properties of PP/ABS blends compatibilized with PP-g-acrylic acid", *J. Appl. Polym. Sci.*, vol. 81, issue 7, pp. 1731-1741, 2001.
- [5] C. K. Kum, Y.-T. Sung, Y. S. Kim, H. G. Lee, W. N. Kim, H. S. Lee, H. G. Yoon, "Effects of Compatibilizer on Mechanical, Morphological, and Rheological Properties of Polypropylene/Poly(acrylonitrile-butadiene-styrene) Blends", *Macromol. Res.*, vol. 15, no. 4, pp. 308-314, 2007.
- [6] P. Xiang-Fang, P. Jun, X. Xiao-li, T. Lih-Sheng, "Effect of organoclay on the mechanical properties and crystallization behaviors of injection-molded PP/ABS/montmorillonitenanocomposites", *ANTEC conference proceedings*, pp. 1105-1108, 2009.
- [7] I. Nigam, D. Nigam, G. N. Marthur, "Effect of Rubber Content of ABS on Properties of PC/ABS Blends. I. Rheological, Mechanical, and Thermal Properties", *Polym.-Plast. Technol. Eng.*, vol. 44, issue 5, pp. 815-832, 2005.
- [8] A. C. Patel, R. B. Brahmabhatt, S. Devi, "Mechanical properties and morphology of PP/ABS blends compatibilized with PP-g-2-HEMA", *J. Appl. Polym. Sci.*, vol. 88, issue 1, pp. 72-78, 2003.
- [9] Y. Wang, Q. Zhang, Q. Fu, "Compatibilization of Immiscible Poly(propylene)/Polystyrene Blends Using Clay", *Macromol. Rapid Commun.*, vol. 24, issue 3, pp. 231-235, 2003.
- [10] B. Chen, J. R. G. Evans, "Mechanical properties of polymer-blend nanocomposites with organoclays: Polystyrene/ABS and high impact polystyrene/ABS", *J. Polym. Sci., Part B: Polym. Phys.*, vol. 49, issue 6, pp. 443-454, 2011.
- [11] C. C. Ibeh, N. Baker, D. Lamm, S. Wang, D. Weber, J. Oplonitnik, *ANTEC conference proceedings* 5, pp. 1893-1897, 2005.
- [12] Y. T. Sung, Y. S. Kim, Y. K. Lee, W. N. Kim, H. S. Lee, J. Y. Sung, H. G. Yoon, "Effects of clay on the morphology of Poly(acrylonitrile-butadiene-styrene) and polypropylene nanocomposites", *Polym. Eng. Sci.*, vol. 47, issue 10, pp. 1671-1677, 2007.
- [13] Q. Shu, X. Zou, W. Dai, Z. Fu, "Formation of  $\beta$ -iPP in isotactic polypropylene/acrylonitrile-butadiene-styrene blends: Effect of resin type, phase composition, and thermal condition", *J. Macromol. Sci., Part B: Phys.*, vol. 51, pp. 756-766, 2012.
- [14] C. Wang, Z. Zhang, Y. Du, J. Zhang, K. Mai, "Effect of acrylonitrile-butadiene-styrene copolymer(ABS) on  $\beta$ -nucleation in  $\beta$ -nucleated polypropylene/ABS blends", *Polym. Bull.*, vol. 69, pp. 847-859, 2012.
- [15] Y. Cai, F. Huang, X. Xia, Q. Wei, X. Tong, A. Wie, W. Gao, "Comparison between structures and properties of ABS nanocomposites derived from two different kinds of OMT", *J. Mater. Eng. Perform.*, vol. 19, pp. 171-176, 2010.
- [16] H. Ma, L. Tong, Z. Xu, Z. Fang, "Clay network in ABS-graft-MAH nanocomposites: rheology and flammability", *Polym. Degrad. Stab.*, vol. 92, pp. 1439-1445, 2007.